

SCIENTIFIC REPORTS



OPEN

Initial evenness determines diversity and cell density dynamics in synthetic microbial ecosystems

Elham Ehsani¹, Emma Hernandez-Sanabria¹, Frederiek-Maarten Kerckhof¹, Ruben Props¹, Ramiro Vilchez-Vargas¹, Marius Vital², Dietmar H. Pieper² & Nico Boon¹

The effect of initial evenness on the temporal trajectory of synthetic communities in comprehensive, low-volume microcosm studies remains unknown. We used flow cytometric fingerprinting and 16S rRNA gene amplicon sequencing to assess the impact of time on community structure in one hundred synthetic ecosystems of fixed richness but varying initial evenness. Both methodologies uncovered a similar reduction in diversity within synthetic communities of medium and high initial evenness classes. However, the results of amplicon sequencing showed that there were no significant differences between and within the communities in all evenness groups at the end of the experiment. Nevertheless, initial evenness significantly impacted the cell density of the community after five medium transfers. Highly even communities retained the highest cell densities at the end of the experiment. The relative abundances of individual species could be associated to particular evenness groups, suggesting that their presence was dependent on the initial evenness of the synthetic community. Our results reveal that using synthetic communities for testing ecological hypotheses requires prior assessment of initial evenness, as it impacts temporal dynamics.

Microbial communities, where cells interact and communicate with one another and influence each other's behaviour, are dynamic change agents in numerous ecosystems^{1,2}. Comprehensive understanding of community properties such as diversity and structure is currently insufficient and, consequently, the description of natural communities remains challenging^{3,4}. Uncovering functional and/or active members of natural microbial communities is a complex task. Hence, model systems have been developed. Synthetic communities are simplified representations of natural ecosystems, with improved reproducibility⁵ in a controlled environment^{6,7}. These have been applied to study microbial interactions and biodiversity-production relationships^{8,9}. For instance, for bioethanol production^{10,11}, bioremediation of contaminated areas¹², recycling of waste products during long distance space exploration¹³, and as an alternative for human faecal transplants¹⁴.

The impact of diversity, richness, and evenness on ecosystem functions such as stress resistance, invasion, and predation interactions^{15–17} has been reported. Although evenness influences community dynamics^{18,19}, the stability of synthetic communities with different initial evenness over time is yet to be elucidated. In this study, we monitored the progress of communities with different initial evenness, and we hypothesized that these communities evolve in a similar and simultaneous fashion. A previous report showed that initial community evenness is a key factor for preserving the stability of an ecosystem¹⁷. Hence, extensive characterization of the evolving community structure is essential for a comprehensive overview of this process.

Currently, microbial community structure and dynamics are often determined based on 16S rRNA gene amplicon sequencing, which remains the standard method for culture-independent surveys of microbial diversity. On the other hand, flow cytometry (FCM) couples high accuracy with sensitivity, ranging from a single cell level to the community level²⁰. FCM is a fast, high throughput method with a wide variety of potential applications, particularly in medical research and microbial ecology. Nonetheless, it is mostly limited to liquid samples and only partial information on community structure can be obtained from this analysis²¹. Flow cytometry fingerprinting (FCFP) is a promising approach to monitor complex microbial communities and to detect changes in the structure of communities. FCFP was applied to estimate the biodiversity of microbial communities, using a phenotypic diversity index based on single cell phenotypic characteristics, such as morphology and nucleic

¹Center for Microbial Ecology and Technology (CMET), Coupure Links 653, 9000 Ghent, Belgium. ²Microbial Interactions and Processes Research Group, Helmholtz Centre for Infection Research, Inhoffenstr. 7, Braunschweig, 38124, Germany. Correspondence and requests for materials should be addressed to N.B. (email: Nico.Boon@UGent.be)

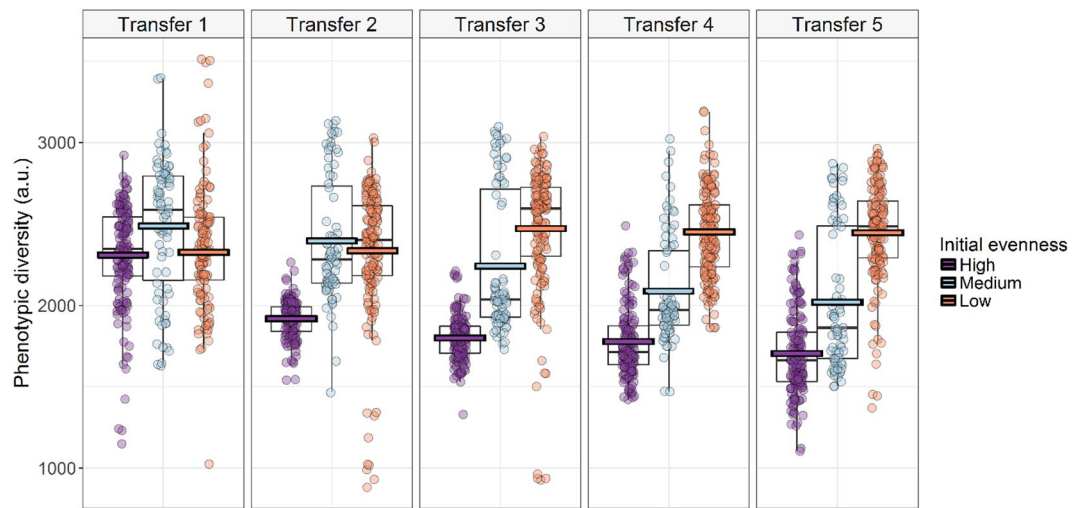


Figure 1. Phenotypic diversity (D_2) dynamics for all microbial communities between transfer 1 (48 h) to 5 (240 h), calculated based on the flow cytometry data ($n = 1913$). Colored horizontal bars indicate the predicted mean from the generalized linear mixed model.

Evenness	Transfer	Mean					
		Pielou	Shannon	Simpson	Fisher's Alpha	Inverse Simpson	Total species
High	0	0.68 ^a	1.56 ^a	0.71 ^a	1.25 ^a	3.81 ^a	10
Medium	0	0.55 ^b	1.24 ^b	0.60 ^{bc}	1.20 ^{ab}	2.81 ^{bc}	10
Low	0	0.60 ^b	1.32 ^b	0.65 ^b	1.14 ^b	3.18 ^b	9
High	5	0.57 ^{cb}	1.03 ^{cb}	0.54 ^c	0.73 ^c	2.30 ^d	6
Medium	5	0.58 ^{cb}	1.05 ^c	0.56 ^c	0.73 ^c	2.35 ^{cd}	6
Low	5	0.57 ^{cb}	1.03 ^c	0.55 ^c	0.74 ^c	2.35 ^{cd}	6
<i>P</i> value							
Evenness		0.03	0.006	0.16	0.05	0.008	0.06
Transfer		0.06	<0.0001	<0.0001	<0.0001	<0.0001	<0.0001
Evenness*Transfer		0.03	0.003	0.02	0.001	0.002	0.002

Table 1. Differences in diversity and evenness indices between transfers 0 (0 h) and 5 (240 h). Different superscripts within column indicate significantly different means ($n = 100$).

acid content²⁰, but has not been used in synthetic communities previously. Additionally, FCM and sequencing techniques have been applied together to gain insight into community structure and dynamics over time^{22–28}. In contrast with these studies, which surveyed natural communities, we monitored the temporal trajectory of synthetic communities. For these reasons, we employed complementary techniques to survey the community evolution of synthetic communities.

In this study, we assembled 100 different synthetic communities with the same richness but different initial evenness. We then combined flow cytometric fingerprinting and amplicon sequencing of the 16S rRNA gene, to monitor how initial evenness variations induced different temporal dynamics in community structure at the taxonomic and physiological level. Understanding these variations can assist us in recognising critical time points for community stability and resilience, which may be potentially modulated in synthetic microbial communities.

Results

Phenotypic diversity and total cell counts fluctuate over time. Shifts in community structure were monitored in one hundred microcosms with same richness but varying initial evenness (divided into low, medium or high evenness group). Each synthetic community was sampled before a medium transfer that occurred at five discrete time points (at 48 h, 96 h, 144 h, 192 h, and 240 h). A transfer consisted of inoculating five percent of the liquid microcosm into fresh medium, (48 h). A total of 1913 observations were recorded and a significant decrease in the phenotypic diversity (Hill order 2) ($P < 0.001$) in high and medium evenness groups was observed, following flow cytometric fingerprinting. Conversely, there was no significant difference ($P = 0.18$) in the low evenness group (Fig. 1 and Supplementary Figure S1). Cell numbers and phenotypic diversity were measured at the end of each subsequent transfer (Fig. 2). The total cell count was not significantly different between medium and high evenness categories, but both groups differed in total cell counts with the low evenness category

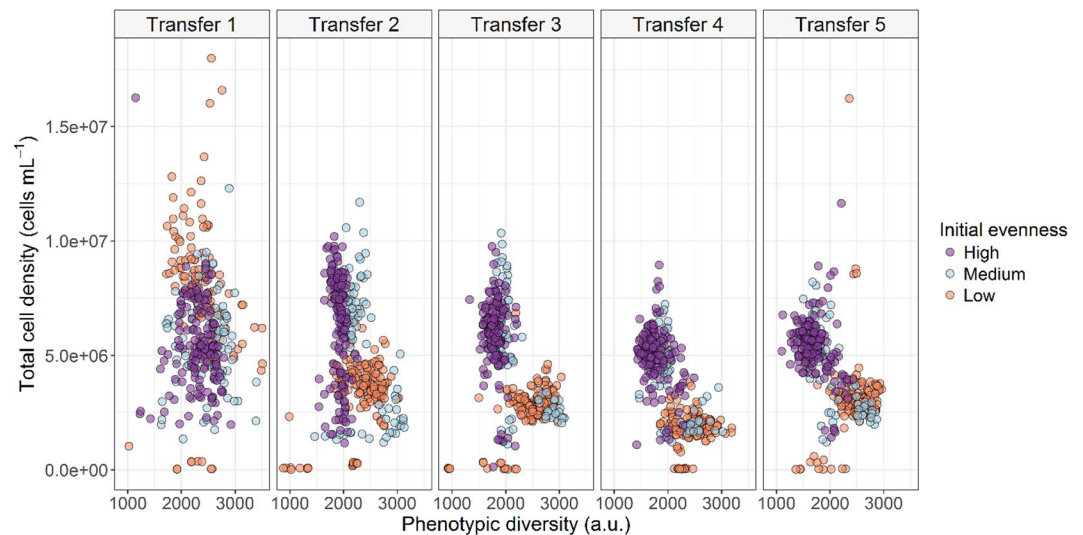


Figure 2. Scatterplot of the total cell density vs. the phenotypic diversity (D_2 , inverse Simpson index) at the end of each subsequent transfer following the initial inoculation.

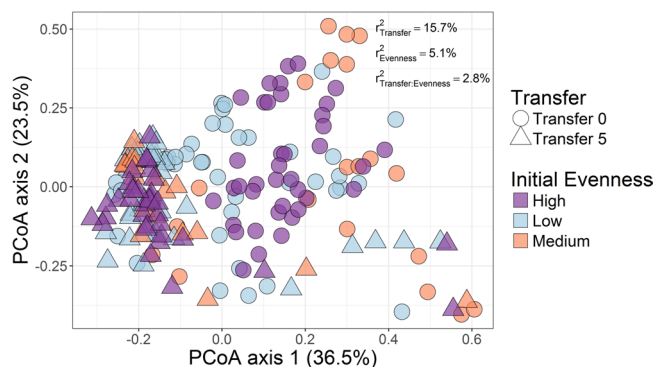


Figure 3. Principal coordinate analysis (PCoA) indicating differences in community structure between transfers 0 (0 h) and 5 (240 h). The variance explained by the experimental factors ($P < 0.01$) is indicated on the top right (PERMANOVA).

at transfer 1. Communities with high initial evenness separated from low and medium evenness groups, and showed higher total cell count and less diversity. Furthermore, mean phenotypic diversity and total cell count were significantly different at transfer 5 between all evenness groups ($P < 0.0001$, Supplementary Table S1).

Community structure converged regardless of initial evenness. 16S rRNA gene amplicon sequencing was performed to validate the phenotypic diversity trends revealed by flow cytometry, and to quantify each member of the synthetic communities at the start of the experiment (transfer 0) and after transfer 5.

Several diversity indices were utilized to describe community composition, structure, and dynamics from the sequencing data. We applied the Fisher's alpha diversity, Shannon–Wiener index, Pielou's Evenness, Simpson's, and inverse Simpson indices in this experiment. All diversity indices excepting for Simpson index were significantly different between transfer 0 and 5. The decrease in diversity was significant in all evenness groups across transfers ($P < 0.05$, Table 1). The evenness showed a decreasing trend between the start and end of the experiment, and the difference was significant ($P < 0.005$) in communities with high initial evenness. The results of different diversity indices were confirmed by measuring three Hill orders (Supplementary Figure S2). *Delftia*, *Aeromonas*, *Serratia* and *Bacillus* were the most abundant bacteria at transfer 5 in all evenness groups. The relative abundances of *Enterococcus* and *Clostridium* were significantly higher in the Low initial evenness group, in comparison with those in the Medium and High evenness groups (Supplementary Figure S3 and Supplementary Table S2). Beta diversity analysis through non-metric multidimensional scaling (nMDS) showed that communities tended to evolve towards the same structure at transfer 5 (Fig. 3). Moreover, permutational multivariate analysis of variance (PERMANOVA) confirmed that evenness did not explain the differences in community composition at the final transfer ($R^2 = 0.03791$, $P = 0.108$). These observations confirmed that alpha and beta diversity were not significantly different within and between the communities of different initial evenness.

Multiple factor analysis (MFA) further explained how the diversity and evenness metrics were associated with the relative abundance of each member of the synthetic community (supplementary Figure S4). Each of the dimensions of the MFA describes the continuous and categorical variables included in the analysis. In our case, the continuous variables were the relative abundances of the bacterial species, and the categorical variable was the initial evenness category. In this way, one categorical variable and continuous variables will compose each dimension. For each categorical factor level (evenness category), a one-way analysis of variance was performed using the coordinates of the samples on the axis belonging to either Low, Medium or High evenness. Then, for each factor level of a category (i.e. Low, Medium or High), a Hotelling T^2 -test was used to compare the average of category with the general average. For instance, the distance from the data point representing the abundance of strain A on the Low evenness category to the corresponding axis was calculated. This distance was compared to the distance from the data point representing the average coordinates of the relative abundance of strain A in the three evenness categories to the same axis. The P value associated to this test was transformed to a normal quantile to assess whether the mean of the category was significantly less or greater than 0. Negative values indicate negative correlations²⁹.

Dimension 1 explained the 28% of the variance, while dimension 2 described 24% of the variance and dimension 3, nearly 14% (Supplementary Table S3). None of these dimensions was significantly associated with either of the three initial evenness categories. However, Dimension 4 explained the 10% of the total variance among microbial communities and included the relative abundances (continuous variable) of species composing communities with high initial evenness (categorical variable, Supplementary Table S3). In this dimension, richness and Fisher diversity index were positively associated between each other ($P < 0.0001$), and both were negatively associated with the relative abundances of *Rhizobium* and *Burkholderia* ($P < 0.01$). Fisher's alpha diversity is an indicator for logarithmic changes in relative abundances. The positive association between richness and Fisher's index indicated that high evenness communities tended to have high richness, but the distribution of these species was skewed. *Enterococcus*, *Aeromonas* and *Clostridium* were the main genera associated with dimension 4, potentially indicating that their relative abundances were associated with communities of high evenness. *Delftia* and *Tissierella* were associated with dimension 5, and therefore, with communities of low evenness.

Discussion

Effect of initial evenness on diversity and cell density dynamics. We monitored how stability and structure of communities with different initial evenness was impacted over time. Synthetic communities with fixed richness but different evenness were assembled and monitored by both 16S rRNA gene sequencing, to assess taxonomic diversity, and FCFP, to evaluate the phenotypic diversity. Changes in community dynamics as well as reduction in diversity were observed over time. Sequencing results revealed a reduction in diversity at transfer 5 relative to transfer 1, leading to equal α - and β -diversity at the final transfer regardless of the initial evenness. However, FCFP indicated that the decrease in diversity was only significant for the initial High and Medium evenness classes. In contrast with the sequencing results, FCM suggested that diversity may become similar but not identical over time.

Environmental filtering occurs when species are unable to tolerate environmental conditions. Based on this concept, the environment acts as a selective force which has effects on the distribution of biodiversity over the world³⁰. The observed changes in evenness in our synthetic communities can also be a result of the microenvironmental conditions in the context of this experiment. Moreover, diversification continues until the maximum number of species that the ecosystem can support (carrying capacity of ecosystem) is reached. When biodiversity attains saturation, interactions can steer elimination of some taxa³¹.

As previously described, FCFP combined with multidimensional and statistical analysis have been used to detect changes in community composition of drinking water^{32,33}. These previously reported results were based on natural communities, but in our experiment, we worked with small synthetic communities. Thus, our communities may not follow the same underlying ecological principles of natural communities, as a result of the synthetic nature of the experiment³⁴.

Dissimilarities observed between the results of FCFP and amplicon sequencing may be as well due to inherent differences among the techniques: FCFP is based on staining nucleic acids of cells in suspension, whereas amplicon sequencing applications focus on rRNA gene hypervariable regions, and some limitations have been found in both techniques. Sequencing errors, difficulties in assessing operational taxonomic units (OTUs) and numerous 16S rRNA gene copies in some species are limitations of 16S rRNA techniques^{35–37}. The phenotypic diversity estimation in our synthetic communities was based on optical features detected by flow cytometry, enabling us to describe the diversity of the synthetic communities across phenotypic characteristics (i.e. morphology and nucleic acid content), which cannot be inferred from molecular techniques. Recent research has shown strong correlation between the phenotypic and taxonomic diversity of natural freshwater communities in both low and high diversity environments^{20,38}. In contrast to the sequencing-based approach, FCFP is fast (<1 h), cheap (<€1 sample⁻¹) and requires only minute sample volumes (<1 mL) thereby allowing high-frequency and non-invasive tracking of sensitive biological processes, such as the feeding of invasive mussel species on bacterioplankton communities³⁸.

However, further validation of FCM assessment of biodiversity in additional natural and synthetic environments is required²⁰. In contrast to previous studies, we did not find a strong correlation between D_0 and D_2 of the phenotypic and taxonomic diversity for synthetic microbial communities (Fig. 4). FCFP successfully tracked changes between evenness classes in comparison with 16S amplicons sequencing at transfer 5. 16S amplicon sequencing is a standard metric of diversity in the field but it was not suitable for quantifying the relative species abundance in our system. Any PCR-based sequencing method is prone to biases when quantifying diversity, as result of extraction, PCR, issues during annotation, among others. This became evident when comparing the theoretical initial diversity with the 16S rRNA gene amplicon sequencing diversity assessment (Supplementary

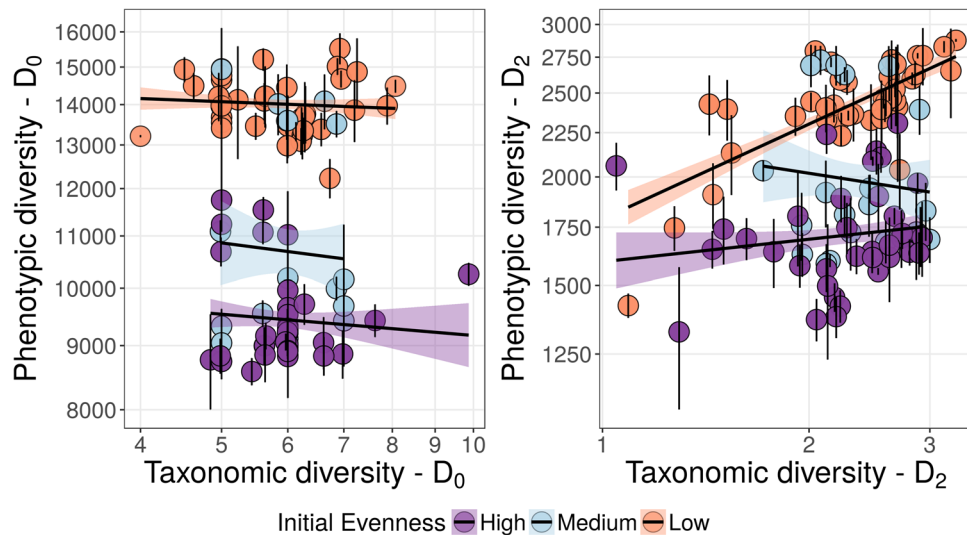


Figure 4. Correlation between D_0 and D_2 of the phenotypic and taxonomic diversity. Flow cytometric fingerprinting diversity as opposed to taxonomic diversity based on diversity order 0 (left panel) and flow cytometric fingerprinting diversity as compared to taxonomic diversity based on diversity order 2 (right panel) at transfer 5.

Figure S5). Our findings are however, increasingly being reported in literature, for example, a recent study described difficulties associated with correcting abundance biases in 16S amplicon data sets³⁹.

Moreover, FCFP showed that the phenotypic diversity tended to be low when bacterial cell numbers were high in all our evenness groups. Thus, communities with low and medium initial evenness were more diverse and had lower total cell counts than communities with high initial evenness. Communities with high initial evenness showed higher cell numbers but low diversity. Milici *et al.* reported a negative correlation between diversity and bacterial cell numbers, suggesting that this may be a result of transient changes in environmental conditions⁴⁰. Our results are also in agreement with the recently proposed hypothesis that microbes adhere to macro-ecological scaling laws, where evenness (diversity) decreases with increasing population size⁴¹. Zhang *et al.* implied that the probability of ecological drifts associated with birth and death, and fluctuations in relative population abundance decrease when there are smaller populations and lower growth rates, which may be the case in our synthetic communities. Thus, it was expected that diversity and bacterial abundance decreased concurrently⁴².

Based upon individual growth curves (data not shown), all strains should have reached stationary phase in between each transfer (i.e. <48 h). Single cells possess traits that increase group performance but that may be detrimental for individual cells⁴³. For instance, fast growth may be inefficient, thereby impacting heterotrophic cell metabolism and ultimately entire population density⁴⁴. In contrast, higher yields optimize limited environmental resources, and support the survival of the entire population⁴⁵. Indeed, shifts between mixed and segregated cell lineages affect the evolution of cooperative and antagonistic phenotypes⁴⁶. In natural settings, community members may differ in the level of cooperation, which makes social interaction open to exploitation⁴³. For instance, *P. aeruginosa* delays investment into cooperation when its impact on fitness becomes negligible⁴⁷. We artificially altered the fitness of certain strains by initially mixing the strains at different ratios. In this way, the differences in the evenness among communities may have triggered competitive interactions that ultimately drove the community to a low cell density. In addition, Zha *et al.* reported that evenness increased with increasing dispersal rates. It is possible that the repeated inoculation in our experiment may have had a similar effect⁴⁸.

Our results showed a fluctuation of cell density over time in all communities. Thus, the effect of initial evenness on cell density after five subsequent transfers for the Low and Medium initial evenness categories was uncovered. Cell density decreased in all groups but communities with low initial evenness showed the fastest decrease over time. Communities with high initial evenness retained a higher cell density over time in comparison with other groups. The results at the final transfer in all evenness groups indicated that *Bacillus*, *Rhizobium* and *Burkholderia* had very low abundances in the Low evenness group, whereas *Rhizobium* and *Burkholderia* were almost absent in the Medium group. Therefore, higher cell numbers at the final transfer in the High evenness group may be due to the presence of all species, as indicated by the sequencing results.

Implications of initial evenness for synthetic microbial community experiments. Knowledge of differences between communities is essential for identifying ecosystem dynamics. For instance, Wittebolle *et al.* proposed that communities with high initial evenness may present improved resistance during environmental oscillations, by creating specialized microcosms with varying evenness without changing richness. Communities with high initial evenness showed higher functional stability even under non-stressed conditions in comparison with those with low initial evenness¹⁷. Importantly, most synthetic community studies did not fully control for potentially evenness-dependent temporal effects on community diversity, function, and cell density. Understanding cooperative and competitive interactions assists to clarify community function, assembly, and

Phylum	ID	Isolated site	Closest taxonomic identifier (NCBI ID)
α Proteobacteria	<i>Rhizobium sp.</i>	soil & water contaminated with alkanes	<i>Rhizobium daejeonense</i>
β Proteobacteria	<i>Delftia sp.</i>	soil & water contaminated with alkanes	<i>Delftia acidovorans</i>
	<i>Burkholderia sp.</i>	soil & water contaminated with alkanes	<i>Burkholderia xenovorans</i>
γ Proteobacteria	<i>Aeromonas sp.</i> ^a	Sand filter	<i>Aeromonas sp. EERV15</i>
	<i>Serratia sp.</i>	soil & water contaminated with alkanes	<i>Serratia myotis</i>
Firmicutes	<i>Enterococcus sp.</i>	soil & water contaminated with alkanes	<i>Enterococcus gallinarum</i>
	<i>Bacillus sp. (Bacillus I)</i>	soil & water contaminated with alkanes	<i>Bacillus methylotrophicus</i>
	<i>Clostridium sp.</i>	soil & water contaminated with alkanes	<i>Clostridium bifermentans</i>
	<i>Tissierella sp.</i>	soil & water contaminated with alkanes	<i>Tissierella sp. FSAA-15</i>
	<i>Bacillus sp.</i>	soil & water contaminated with alkanes	<i>Bacillus mycoides</i>

Table 2. Strains used to create the microcosms with different degrees of initial evenness. ^aDraft genome is available⁶⁶.

stability. Collaborations within and among bacterial communities can arise when one or a group of species provide nutrition or protection to another, whereas competition occurs when some species compete for a shared metabolite⁴⁹. In the context of this experiment, *Bacillus*, *Enterococcus*, *Aeromonas*, and *Clostridium* were associated with low evenness whereas *Delftia* and *Tissierella* were correlated with high evenness, suggesting that they are more abundant on either group. Therefore, *Delftia* and *Tissierella* thrived in our communities with High evenness, while *Aeromonas* and *Enterococcus* succeed in the communities designed with Low evenness. *Aeromonas* abundance was negatively correlated with *Delftia*, *Serratia* and *Enterococcus* abundance but positively correlated with *Bacillus* abundance. Thus, *Serratia* and *Enterococcus* were less present in communities with high relative abundance of *Aeromonas*. *Burkholderia* and *Rhizobium* were correlated with each other positively, which may explain their consistent low relative abundance in all the evenness groups.

Understanding how community structure changes over time is a fundamental question in ecology. The structure and composition of natural microbial communities remains to be elucidated because of the presence of non-cultivable species. The complete description of their functions and microbial interactions remains challenging. Unlike temporal dynamics of animal and plant communities, the temporal dynamics exhibited by microbial communities have not been fully described⁵⁰. Based on our results, the combined use of FCM and sequencing provided an overview of community structure dynamics, allowing for efficient monitoring of natural microbial communities. Synthetic communities are of special interest, because description of their characteristics has not been performed yet. Knowledge of these traits will assist us to elucidate the effect of time on community stability and resilience, which are key functional characteristics of microbial communities. Using synthetic and controlled microbial communities may also further our mechanistic understanding and support the development of models with increased predictive power. In the context of our study, deterministic selection may have impacted the population size over time. This finding may be relevant for the development of engineered communities with targeted functionality, such as those in wastewater treatment or environmental bioremediation. By monitoring diversity, structure, resilience and stability of communities, bioremediation efficiency⁵¹ may be predicted, for instance, and successful *in situ* bioremediation techniques can be implemented⁵².

Methods

Construction of synthetic communities. A total of 10 environmental bacterial species from 4 phyla (Table 2) were mixed in different proportions to create microcosms with varying evenness but with the same number of species (richness). We quantified initial evenness using the Pielou index, which is an excellent measure for community structure. This metric encapsulates the component of species richness within an ecosystem, as well as the species distribution, and it is rescaled between 0 (most uneven community) and 1 (completely even)^{53,54}. In this way, the synthetic communities were grouped in Low, Medium, and High evenness (between 0–0.3, 0.4–0.6 and 0.6–1 respectively), based on their initial Pielou evenness. One hundred synthetic communities were sampled from an experimental design of one million *in silico* simulated synthetic communities (supplementary information: experimental design section and Supplementary Table S4). The 100 different communities were distributed between the evenness classes: 40 microcosms with low, 20 with medium and 40 microcosms with high evenness. For this purpose, 96 deep well microtiter plates were filled with 2 ml of fresh LB medium and 5% (v/v) of the microcosms, with adjacent duplicates of each mixture. Subsequently, these plates were incubated at 28 °C on a microplate shaker at 250 rpm. After 48 h, 5% of the community was transferred to another microplate with fresh medium and incubated for 48 h. This procedure was repeated five times, i.e. for a total of 240 h. Cell number and community phenotypic diversity were assessed after each transfer (at 48 h, 96 h, 144 h, 192 h, and 240 h) by means of flow cytometry (Accuri C6 Flow cytometer, BD Biosciences, Erembodegem, Belgium), with SYBR green I staining of the nucleic acids as described by De Roy *et al.*⁵. Further, amplicon sequencing of the 16S rRNA genes (Illumina Miseq, Illumina, Hayward, CA, USA) was performed at transfer 0 and 5 to supplement the results of FCFP.

Cell number and phenotypic characteristics assessment. Synthetic communities were diluted (1,000, 5,000 or 10,000 times) in 145 mM of NaCl and stained with SYBR Green I to determine total cell count^{5,55}. Four technical replicates of each sample were prepared and analysed to obtain robust estimates of the phenotypic

characteristics. The data points belonging to the microbial community were isolated from (in-)organic and instrument noise using a gating strategy applied on the FL1-H and FL3-H channels (Supplementary Figure S6).

Microbial phenotypic diversity was estimated for all samples ($n = 1913$) using a novel computational method, which calculates various diversity estimators based on single-cell phenotypic features²⁰. Nucleic acid content and scatter signals were employed to calculate the phenotypic diversity metrics (i.e. Hill numbers) from these distributions. We utilized the *flowBasis* and *Diversity* functions with default settings on the denoised data, per the protocol available at https://github.com/rprops/Phenoflow_package (v1.0, seed = 777). Samples with less than 1,000 cells were excluded from the analysis, resulting in a minimum sample size of 5,000 cells. We utilized the Hill diversity of order 2, also known as the inverse Simpson index, for inference on community diversity metrics.

DNA extraction. One ml from each community was centrifuged 10 min at $13000 \times g$, supernatant was removed and the pellet was stored immediately at -20°C until further analysis⁵⁶. Cells were lysed with 1 mL of lysis buffer (100 mM Tris/HCl pH 8.0, 100 mM EDTA pH 8, 100 mM NaCl, 1% (m/v) polyvinylpyrrolidone and 2% (m/v) sodium dodecyl sulphate) and 200 mg of glass beads (0.11 mm, Sartorius), in a FastPrep[®] – 96 instrument (MP Biomedicals, Santa Ana, USA), two times for 40 s at 1600 rpm. After removing glass beads by centrifugation (5 min at 13000 g), DNA was extracted following a phenol–chloroform extraction. DNA was precipitated with 1 volume ice-cold isopropyl alcohol and 0.1 volume 3 M sodium acetate for 1 h at -20°C . DNA pellet was dried and resuspended in $100 \mu\text{L}$ $1 \times \text{TE}$ (10 mM Tris, 1 mM EDTA) buffer. Samples were immediately stored at -20°C until further analysis. Quality of DNA was analysed by gel electrophoresis.

16 rRNA gene sequencing and analyses. The V1–V2 hypervariable regions of the 16 S rRNA gene were amplified as described by Camarinha-Silva *et al.*⁵⁷. Sequencing was performed using Illumina MiSeq sequencer and reads were clustered allowing for two mismatches as previously defined⁵⁸. The dataset was then filtered to consider only those phylotypes that were present in at least one sample at a relative abundance $>0.1\%$ or were present in all samples at a relative abundance $>0.001\%$ ⁵⁷. A total of 200 samples were analysed and a total of 6 million reads was obtained. Sequence composition was compared using the RDP Classifier tool⁵⁹ and SILVA database⁶⁰. After examining read counts, data were rarefied to a chosen maximum depth of 3317 sequences, using the phyloseq package from R⁶¹ and rarefaction curves were plotted using the vegan package in R⁶².

Statistical analysis. Alpha diversity was assessed calculating the total number of species, Fisher's diversity, Shannon, Simpson and inverse Simpson indices for all evenness categories (H, L or M) and for transfer, using the vegan software package in R⁶². Pielou's index was used as indicator of evenness in the community. Differences in alpha diversity and evenness measures among transfers and evenness categories were compared using a repeated measures mixed model in SAS (version 9.3, SAS Institute, Cary, USA), and comparing multiple means using Tukey test. In this way, the differences in the diversity measures among communities could be attributed to either evenness category, transfer or to the interaction transfer*evenness category. Hill numbers or effective number of species⁶³ were calculated from amplicon sequencing, as well as from FCM data, using the Phenoflow package. A generalized mixed model was constructed to evaluate the interaction effect between transfer and initial evenness on the phenotypic diversity (*nlme* package)⁶⁴. Random intercepts were included for each biological replicate and autocorrelation was addressed by an AR1 structure. Parameters were estimated using the restricted maximum likelihood approach. Tukey's all pair comparison was conducted for pairwise comparisons between initial evenness groups at each transfer. Normality and homoscedasticity of the model residuals were visually checked using diagnostic plots (Supplementary Figure S1).

Permutational multivariate analysis of variance (PERMANOVA) with 999 permutations was conducted to explore the percentage of variance that could be explained by the differences in beta diversity, based on Bray–Curtis distance matrices. Tukey's test for pairwise comparisons of group mean dispersions was performed using the vegan package in R. Further, the function *adonis* was used to perform a one-way ANOVA, to determine the impact of evenness in community diversity. Differences in relative abundances of the bacterial genera composing each community were compared using a repeated measures mixed model in SAS, with the least squares means adjustment and Bonferroni correction for multiple comparisons⁶⁵. Multiple factor analysis (MFA) was used to reveal whether any of the diversity metrics and/or evenness were associated with each member of the synthetic communities (FactoMineR package)²⁹.

Data availability. The authors declare that the main data supporting the findings of this study are available within the article and its Supplementary Information files. All FCS files of flow cytometry data, accompanying metadata have been deposited to the Flow Repository website with the repository ID FR-FCM-ZYBR (<http://flowrepository.org/id/FR-FCM-ZYBR>). The OTU table (97% identity) also has been added to supplementary information (Supplementary Table S5).

References

- Boon, E. *et al.* Interactions in the microbiome: communities of organisms and communities of genes. *FEMS Microbiol Rev* **38**, 90–118, <https://doi.org/10.1111/1574-6976.12035> (2014).
- Comolli, L. R. Intra- and inter-species interactions in microbial communities. *Front Microbiol* **5**, 629, <https://doi.org/10.3389/fmicb.2014.00629> (2014).
- Prosser, J. I. *et al.* The role of ecological theory in microbial ecology. *Nat Rev Microbiol* **5**, 384–392, <https://doi.org/10.1038/nrmicro1643> (2007).
- Morales, S. E. & Holben, W. E. Linking bacterial identities and ecosystem processes: can 'omic' analyses be more than the sum of their parts? *FEMS Microbiol Ecol* **75**, 2–16, <https://doi.org/10.1111/j.1574-6941.2010.00938.x> (2011).
- De Roy, K., Marzorati, M., Van den Abbeele, P., Van de Wiele, T. & Boon, N. Synthetic microbial ecosystems: an exciting tool to understand and apply microbial communities. *Environ Microbiol* **16**, 1472–1481, <https://doi.org/10.1111/1462-2920.12343> (2014).

6. Grosskopf, T. & Soyer, O. S. Synthetic microbial communities. *Curr Opin Microbiol* **18**, 72–77, <https://doi.org/10.1016/j.mib.2014.02.002> (2014).
7. Tanouhi, B. & Agathos, S. N. Deciphering microbial community robustness through synthetic ecology and molecular systems synecology. *Curr Opin Biotechnol* **33**, 305–317, <https://doi.org/10.1016/j.copbio.2015.03.012> (2015).
8. Klitgord, N. & Segre, D. Environments that induce synthetic microbial ecosystems. *PLoS Comput Biol* **6**, e1001002, <https://doi.org/10.1371/journal.pcbi.1001002> (2010).
9. Tanouchi, Y., Smith, R. P. & You, L. Engineering microbial systems to explore ecological and evolutionary dynamics. *Curr Opin Biotechnol* **23**, 791–797, <https://doi.org/10.1016/j.copbio.2012.01.006> (2012).
10. Chen, Y. Development and application of co-culture for ethanol production by co-fermentation of glucose and xylose: a systematic review. *J Ind Microbiol Biotechnol* **38**, 581–597, <https://doi.org/10.1007/s10295-010-0894-3> (2011).
11. Ma, Q. *et al.* Integrated proteomic and metabolomic analysis of an artificial microbial community for two-step production of vitamin C. *PLoS One* **6**, e26108, <https://doi.org/10.1371/journal.pone.0026108> (2011).
12. Dejonghe, W. *et al.* Synergistic degradation of linuron by a bacterial consortium and isolation of a single linuron-degrading variorax strain. *Appl Environ Microbiol* **69**, 1532–1541 (2003).
13. Hendrickx, L. *et al.* Microbial ecology of the closed artificial ecosystem MELiSSA (Micro-Ecological Life Support System Alternative): reinventing and compartmentalizing the Earth's food and oxygen regeneration system for long-haul space exploration missions. *Res Microbiol* **157**, 77–86, <https://doi.org/10.1016/j.resmic.2005.06.014> (2006).
14. Eckburg, P. B. *et al.* Diversity of the human intestinal microbial flora. *Science* **308**, 1635–1638, <https://doi.org/10.1126/science.1110591> (2005).
15. De Roy, K. *et al.* Environmental conditions and community evenness determine the outcome of biological invasion. *Nat Commun* **4**, 1383, <https://doi.org/10.1038/ncomms2392> (2013).
16. Saleem, M., Fetzer, I., Dormann, C. F., Harms, H. & Chatzinotas, A. Predator richness increases the effect of prey diversity on prey yield. *Nat Commun* **3**, 1305, <https://doi.org/10.1038/ncomms2287> (2012).
17. Wittebolle, L. *et al.* Initial community evenness favours functionality under selective stress. *Nature* **458**, 623–626, <https://doi.org/10.1038/nature07840> (2009).
18. Huber, J. A. *et al.* Microbial population structures in the deep marine biosphere. *Science* **318**, 97–100, <https://doi.org/10.1126/science.1146689> (2007).
19. Werner, J. J. *et al.* Microbial community dynamics and stability during an ammonia-induced shift to syntrophic acetate oxidation. *Appl Environ Microbiol* **80**, 3375–3383, <https://doi.org/10.1128/AEM.00166-14> (2014).
20. Props, R., Monsieurs, P., Mysara, M., Clement, L. & Boon, N. Measuring the biodiversity of microbial communities by flow cytometry Methods in Ecology and Evolution Accepted Article. *Methods in Ecology and Evolution*, n/a <http://onlinelibrary.wiley.com/doi/10.1111/2041-210X.12607/abstract> (2016).
21. Wang, Y., Hammes, F., De Roy, K., Verstraete, W. & Boon, N. Past, present and future applications of flow cytometry in aquatic microbiology. *Trends Biotechnol* **28**, 416–424, <https://doi.org/10.1016/j.tibtech.2010.04.006> (2010).
22. Liu, T. *et al.* Bacterial characterization of Beijing drinking water by flow cytometry and MiSeq sequencing of the 16S rRNA gene. *Ecol Evol* **6**, 923–934, <https://doi.org/10.1002/ece3.1955> (2016).
23. El-Chakhtoura, J. *et al.* Dynamics of bacterial communities before and after distribution in a full-scale drinking water network. *Water Res* **74**, 180–190, <https://doi.org/10.1016/j.watres.2015.02.015> (2015).
24. Prest, E. I. *et al.* Combining flow cytometry and 16S rRNA gene pyrosequencing: a promising approach for drinking water monitoring and characterization. *Water Res* **63**, 179–189, <https://doi.org/10.1016/j.watres.2014.06.020> (2014).
25. Bombach, P. *et al.* Resolution of natural microbial community dynamics by community fingerprinting, flow cytometry, and trend interpretation analysis. *Adv Biochem Eng Biotechnol* **124**, 151–181, https://doi.org/10.1007/10_2010_82 (2011).
26. Hoefel, D., Monis, P. T., Grooby, W. L., Andrews, S. & Saint, C. P. Profiling bacterial survival through a water treatment process and subsequent distribution system. *J Appl Microbiol* **99**, 175–186, <https://doi.org/10.1111/j.1365-2672.2005.02573.x> (2005).
27. Kinet, R. *et al.* Flow cytometry community fingerprinting and amplicon sequencing for the assessment of landfill leachate cellulolytic bioaugmentation. *Bioresour Technol* **214**, 450–459, <https://doi.org/10.1016/j.biortech.2016.04.131> (2016).
28. Props, R. *et al.* Absolute quantification of microbial taxon abundances. *ISME J*, <https://doi.org/10.1038/ismej.2016.117> (2016).
29. Le, S., Josse, J. & Husson, F. FactoMineR: An R Package for Multivariate Analysis. *JSS Journal of Statistical Software* **25**, 1–18 (2008).
30. Kraft, N. J. B. *et al.* Community assembly, coexistence and the environmental filtering metaphor Functional Ecology Volume 29, Issue 5. *Functional Ecology* **29**, 592–599, <https://doi.org/10.1111/1365-2435.12345/abstract> (2015).
31. Monte-Luna, P. D., Brook, B. W., Zetina-Rejón, M. J. & Cruz-Escalona, V. H. The carrying capacity of ecosystems Global Ecology and Biogeography Volume 13, Issue 6. *Global Ecology and Biogeography* **13**, 485–495, <https://doi.org/10.1111/j.1466-822X.2004.00131.x/abstract> (2004).
32. Bergquist, P. L., Hardiman, E. M., Ferrari, B. C. & Winsley, T. Applications of flow cytometry in environmental microbiology and biotechnology. *Extremophiles* **13**, 389–401, <https://doi.org/10.1007/s00792-009-0236-4> (2009).
33. De Roy, K., Clement, L., Thas, O., Wang, Y. & Boon, N. Flow cytometry for fast microbial community fingerprinting. *Water Res* **46**, 907–919, <https://doi.org/10.1016/j.watres.2011.11.076> (2012).
34. Yu, Z., Krause, S. M., Beck, D. A. & Chistoserdova, L. A Synthetic Ecology Perspective: How Well Does Behavior of Model Organisms in the Laboratory Predict Microbial Activities in Natural Habitats? *Front Microbiol* **7**, 946, <https://doi.org/10.3389/fmicb.2016.00946> (2016).
35. Poretsky, R., Rodriguez, R. L., Luo, C., Tsementzi, D. & Konstantinidis, K. T. Strengths and limitations of 16S rRNA gene amplicon sequencing in revealing temporal microbial community dynamics. *PLoS One* **9**, e93827, <https://doi.org/10.1371/journal.pone.0093827> (2014).
36. DePristo, M. A. *et al.* A framework for variation discovery and genotyping using next-generation DNA sequencing data. *Nat Genet* **43**, 491–498, <https://doi.org/10.1038/ng.806> (2011).
37. Schmidt, T. S. B., Rodrigues, J. F. M. & von Mering, C. Limits to robustness and reproducibility in the demarcation of operational taxonomic units. *Environ Microbiol* **17**, 1689–1706 (2015).
38. Props, R. *et al.* Flow cytometric monitoring of bacterioplankton phenotypic diversity predicts high population-specific feeding rates by invasive dreissenid mussels. *Environmental Microbiology*, In Press, <https://doi.org/10.1111/1462-2920.13953> (2017).
39. Edgar, R. C. UNBIAS: An attempt to correct abundance bias in 16S sequencing, with limited success. *bioRxiv*, 124149 (2017).
40. Milici, M. *et al.* Low diversity of planktonic bacteria in the tropical ocean. *Sci Rep* **6**, 19054, <https://doi.org/10.1038/srep19054> (2016).
41. Locey, K. J. & Lennon, J. T. Scaling laws predict global microbial diversity. *Proc Natl Acad Sci USA* **113**, 5970–5975, <https://doi.org/10.1073/pnas.1521291113> (2016).
42. Zhang, W. *et al.* Modeling the Biodegradation of Bacterial Community Assembly Linked Antibiotics in River Sediment Using a Deterministic-Stochastic Combined Model. *Environ Sci Technol* **50**, 8788–8798, <https://doi.org/10.1021/acs.est.6b01573> (2016).
43. Xavier, J. B. Social interaction in synthetic and natural microbial communities. *Mol Syst Biol* **7**, 483, <https://doi.org/10.1038/msb.2011.16> (2011).
44. Pfeiffer, T., Schuster, S. & Bonhoeffer, S. Cooperation and competition in the evolution of ATP-producing pathways. *Science* **292**, 504–507, <https://doi.org/10.1126/science.1058079> (2001).

45. Pfeiffer, T. & Bonhoeffer, S. An evolutionary scenario for the transition to undifferentiated multicellularity. *Proc Natl Acad Sci USA* **100**, 1095–1098, <https://doi.org/10.1073/pnas.0335420100> (2003).
46. Nadell, C. D., Drescher, K. & Foster, K. R. Spatial structure, cooperation and competition in biofilms. *Nat Rev Microbiol* **14**, 589–600, <https://doi.org/10.1038/nrmicro.2016.84> (2016).
47. Xavier, J. B., Kim, W. & Foster, K. R. A molecular mechanism that stabilizes cooperative secretions in *Pseudomonas aeruginosa*. *Mol Microbiol* **79**, 166–179, <https://doi.org/10.1111/j.1365-2958.2010.07436.x> (2011).
48. Zha, Y., Berga, M., Comte, J. & Langenheder, S. Effects of Dispersal and Initial Diversity on the Composition and Functional Performance of Bacterial Communities. *PLoS One* **11**, e0155239, <https://doi.org/10.1371/journal.pone.0155239> (2016).
49. Freilich, S. *et al.* Competitive and cooperative metabolic interactions in bacterial communities. *Nat Commun* **2**, 589, <https://doi.org/10.1038/ncomms1597> (2011).
50. Shade, A., Caporaso, J. G., Handelsman, J., Knight, R. & Fierer, N. A meta-analysis of changes in bacterial and archaeal communities with time. *ISME J* **7**, 1493–1506, <https://doi.org/10.1038/ismej.2013.54> (2013).
51. Whiteley, A. S. & Bailey, M. J. Bacterial community structure and physiological state within an industrial phenol bioremediation system. *Appl Environ Microbiol* **66**, 2400–2407 (2000).
52. Sarkar, J. *et al.* Biostimulation of Indigenous Microbial Community for Bioremediation of Petroleum Refinery Sludge. *Front Microbiol* **7**, 1407, <https://doi.org/10.3389/fmicb.2016.01407> (2016).
53. Zhang, H. *et al.* The relationship between species richness and evenness in plant communities along a successional gradient: a study from sub-alpine meadows of the Eastern Qinghai-Tibetan Plateau, China. *PLoS One* **7**, e49024, <https://doi.org/10.1371/journal.pone.0049024> (2012).
54. Jost, L. The relation between evenness and diversity. *Diversity* **2**, 207–232 (2010).
55. Van Nevel, S., Koetzsch, S., Weilenmann, H. U., Boon, N. & Hammes, F. Routine bacterial analysis with automated flow cytometry. *J Microbiol Methods* **94**, 73–76, <https://doi.org/10.1016/j.mimet.2013.05.007> (2013).
56. Vilchez-Vargas, R. *et al.* Analysis of the microbial gene landscape and transcriptome for aromatic pollutants and alkane degradation using a novel internally calibrated microarray system. *Environ Microbiol* **15**, 1016–1039, <https://doi.org/10.1111/j.1462-2920.2012.02752.x> (2013).
57. Camarinha-Silva, A. *et al.* Comparing the anterior nares bacterial community of two discrete human populations using Illumina amplicon sequencing. *Environ Microbiol* **16**, 2939–2952, <https://doi.org/10.1111/1462-2920.12362> (2014).
58. Verstraelen, H. *et al.* Characterisation of the human uterine microbiome in non-pregnant women through deep sequencing of the V1-2 region of the 16S rRNA gene. *PeerJ* **4**, e1602, <https://doi.org/10.7717/peerj.1602> (2016).
59. Wang, Q., Garrity, G. M., Tiedje, J. M. & Cole, J. R. Naive Bayesian classifier for rapid assignment of rRNA sequences into the new bacterial taxonomy. *Appl Environ Microbiol* **73**, 5261–5267, <https://doi.org/10.1128/AEM.00062-07> (2007).
60. Pruesse, E. *et al.* SILVA: a comprehensive online resource for quality checked and aligned ribosomal RNA sequence data compatible with ARB. *Nucleic Acids Res* **35**, 7188–7196, <https://doi.org/10.1093/nar/gkm864> (2007).
61. McMurdie, P. J. & Holmes, S. phyloseq: an R package for reproducible interactive analysis and graphics of microbiome census data. *PLoS One* **8**, e61217, <https://doi.org/10.1371/journal.pone.0061217> (2013).
62. Oksanen, J., Kindt, R., Legendre, P., O'Hara, B. & Simpson, G. L. The vegan package. *Community ecology package*, 631–637 (2007).
63. Hill, M. O. Diversity and evenness: a unifying notation and its consequences. *Ecology* **54**, 427–432 (1973).
64. Pinheiro, J. & Bates, D. Mixed Effects Models in S and S-PLUS. *Springer* (2000).
65. Grunert, O. *et al.* Mineral and organic growing media have distinct community structure, stability and functionality in soilless culture systems. *Sci Rep* **6**, 18837, <https://doi.org/10.1038/srep18837> (2016).
66. Ehsani, E. *et al.* Draft Genome Sequence of *Aeromonas* sp. Strain EERV15. *Genome Announc* **4**, <https://doi.org/10.1128/genomeA.00811-16> (2016).

Acknowledgements

This work was funded by a Geconcerteerde Onderzoeksacties (GOA) research grant from Ghent University (BOF15/GOA/006) and the Inter-University Attraction Pole (IUAP) μ -manager financed by the Belgian Science Policy (BELSPO) (grant P7/25). E.H.-S. was supported by the Research Foundation of Flanders (Fonds Wetenschappelijk Onderzoek-Vlaanderen, FWO). The authors also acknowledge Wai Kit Tsang for creating and designing synthetic communities.

Author Contributions

The experiment was originally conceived by E.E., R.V.-V. and N.B. Laboratory work was conducted by E.E. Illumina libraries processing was performed by M.V. and R.V.-V. FCFP and data mining was performed by R.P. and F.-M.K. Interpretation and statistical analyses of sequencing results were implemented by E.H.-S. Reagents/materials/analysis tools were supplied by N.B. and D.H.P. The manuscript was written by E.E., E.H.-S., F.-M.K., and R.P. All the authors read and approved the manuscript.

Additional Information

Supplementary information accompanies this paper at <https://doi.org/10.1038/s41598-017-18668-1>.

Competing Interests: The authors declare that they have no competing interests.

Publisher's note: Springer Nature remains neutral with regard to jurisdictional claims in published maps and institutional affiliations.



Open Access This article is licensed under a Creative Commons Attribution 4.0 International License, which permits use, sharing, adaptation, distribution and reproduction in any medium or format, as long as you give appropriate credit to the original author(s) and the source, provide a link to the Creative Commons license, and indicate if changes were made. The images or other third party material in this article are included in the article's Creative Commons license, unless indicated otherwise in a credit line to the material. If material is not included in the article's Creative Commons license and your intended use is not permitted by statutory regulation or exceeds the permitted use, you will need to obtain permission directly from the copyright holder. To view a copy of this license, visit <http://creativecommons.org/licenses/by/4.0/>.

© The Author(s) 2017